Title
NUCLEAR ORIENTATION OP 2.3-d GOLD-198m

Authors
Mahnke, H.-E.
Kaindl, G.
Bacon, F.
et al.

Publication Date
1975

Submitted to Nuclear Physics A

LBL-3484
Preprint c.1

NUCLEAR ORIENTATION OF 2.3-d GOLD-198m

H.-E. Mahnke, G. Kaindl, F. Bacon, and D. A. Shirley

January 1975

Prepared for the U. S. Atomic Energy Commission
under Contract W-7405-ENG-48

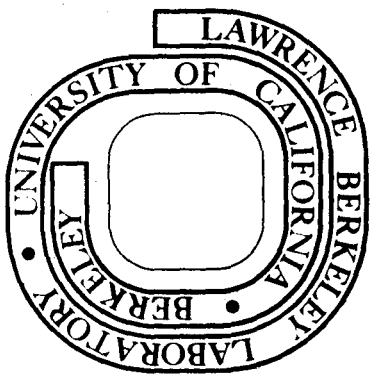

DISCLAIMER

Nuclear Orientation of 2.3-d Gold-198m*

H.-E. Mahnke,† G. Kaindl,‡ F. Bacon,§ and D. A. Shirley

Department of Chemistry and Lawrence Berkeley Laboratory
University of California, Berkeley, California 94720

January 1975

Abstract

The magnetic hyperfine interaction of the $T_{1/2}$ = 2.3-d high-spin isomeric state of ^{198}Au has been measured in host metals of iron and nickel at temperatures down to 4 mK using the thermal-equilibrium nuclear-orientation technique. The resulting value for the magnetic moment, μ = (+) 5.55±0.35 n.m., strongly supports an interpretation of this state as a $\left[\pi h_{11/2};\ \nu i_{13/2}\right]$ 12^- configuration analogous to ^{196m}Au and ^{200m}Au. The observed gamma-ray anisotropies are in agreement with the recently proposed decay scheme of ^{198m}Au; for the E2/M1-mixing ratio of the 204-keV gamma transition they result in a value of δ = - 0.10±0.05.

E | Radioactivity ^{198m}Au from ^{198}Pt(d,2n) and ^{196}Pt(α,pn); measured I_γ (Θ,T) in Fe and Ni; deduced μ,δ; enriched targets.

*Work supported by the U. S. Energy Research and Development Administration.

I. Introduction

The excitation energies of the $h_{11/2}$-proton states in odd-mass gold isotopes and of the $i_{13/2}$-neutron states in odd-mass platinum and mercury isotopes are known to be quite low /1/. One may therefore expect the occurrence of relatively low- lying states with $I^{\pi} = 12^-$ in the neighboring even-mass gold isotopes arising from the coupling of these single-particle states. The large spin difference between these isomers and the corresponding ground states should result in half-lives of several hours.

Such an isomer was first found in ^{196}Au with a half-life of 9.7 h and a spin of 12 /2-5/. The size of the magnetic moment of this state, determined by the thermal-equilibrium nuclear-orientation (NO) technique /6/ supports the previously assigned $\left[\pi h_{11/2};\ \nu i_{13/2}\right]\ 12^-$-configuration. In addition, the 18.7-h isomer of ^{200}Au /7,8/ could be identified as the analogous state by determining both its spin and its magnetic moment /9/.

Recently, two groups have reported their results on the decay of a new long-lived isomeric state in ^{198}Au /10,11/, with a half-life of $T_{1/2} = 2.3\pm0.05$ d. In the course of our experiments on ^{200m}Au we also observed this ^{198}Au activity and performed a measurement of its moment by the NO technique; the results of this work are reported here. A preliminary report of our results has been given elsewhere /12/. The results for the magnetic moment of ^{198m}Au reveal its analogy to the 12^--isomers of ^{196}Au and ^{200}Au.

II. Experimental Procedure

The ^{198m}Au activity was produced by the ^{196}Pt(α,pn)^{198m}Au and by the ^{198}Pt(d,2n)^{198m}Au reactions using enriched metallic platinum targets

and 35-MeV α particles or 18-MeV deuterons, respectively, from the LBL-88" cyclotron. The resulting gold activities were separated from the platinum targets by the standard ethyl-acetate separation technique. For the low-temperature nuclear orientation experiments the carrier-free gold activity was electroplated onto iron or nickel foils of 99.999% nominal purity. The samples, together with a matched amount of ^{60}Co activity to be used for thermometry, were then melted several times in a hydrogen atmosphere, rolled, and annealled so that finally foils with a thickness of approximately 20 mg/cm^2 were obtained.

The samples were contact-cooled down to about 4 mK in an adiabatic demagnetization apparatus, using cerium magnesium nitrate (CMN) as a cooling salt. A superconducting Helmholtz pair was employed to magnetize the sample in an external magnetic field of 4 kOe applied parallel to the plane of the foil.

For the measurement of the temperature dependence of gamma-ray anisotropies, gamma-ray spectra were taken with high-resolution Ge(Li) diodes along and perpendicular to the external polarizing field for time spans of 15 minutes as the sample warmed up to approximately 1 K over a typical period of 10 hours. After corrections were made for background and exponential decay, the anisotropies of the different gamma-lines were obtained. The respective lattice temperatures were determined from the anisotropies of the 1173-keV and 1333-keV gamma lines of ^{60}Co. For further details of the experimental technique, see Ref. 9.

III. Experimental Results

The decay scheme of ^{198m}Au, following from the work of Ref. 10 and 11, is shown in Fig. 1. A relatively weak gamma transition with an

energy of 334 keV which also originates from the decay of ^{198m}Au has not been included in this decay scheme.

The activity used for the NO experiments was produced by the ^{196}Pt(α,pn)^{198m}Au reaction. Gamma-ray anisotropies were observed for the 180-keV, 204-keV, 215-keV, and 334-keV gamma lines. Due to intensity problems connected with the absorption and scattering of gamma rays in our apparatus, anisotropies of gamma lines with energies lower than 150 keV were not evaluated. No information could therefore be obtained for the 97-keV gamma transition.

The temperature dependences of the anisotropies of the 204-keV and of the 215-keV gamma rays were measured for iron and nickel metal hosts. In Fig. 2 the reduced intensities, $W(\theta) = I(\theta,T)/I(T \rightarrow \infty)$, of the 215-keV gamma rays observed along ($\theta = 0^{o}$) and perpendicular ($\theta = 90^{o}$) to the external polarizing field are plotted versus the inverse lattice temperature for a sample of ^{198m}Au(Fe). For the 204-keV line the gamma-ray anisotropy was only evaluated for the nickel host due to difficulties in the correction for background caused by a nearby, intense 208-keV gamma line oiriginating from the decay of ^{199}Au. In the nickel host the nuclear orientation of ^{199}Au is negligible even at the lowest temperatures reached in the present experiments, so that the background under the 204-keV line caused by the tail from the 208-keV line should not change with temperature. This would not be the case for iron as a host. In Fig. 3 the reduced intensity of the 204-keV gamma rays emitted from the ^{198m}Au(Ni) source at $\theta = 0^{o}$ is shown as a function of the inverse lattice temperature. As expected from the assigned predominant M1

multipolarity /11/ a large positive anisotropy is observed.

The anisotropies of the 180-keV and 334-keV gamma lines could not be determined quantitatively due to underlying gamma lines at 333 keV and 181 keV, originating from the decay of ^{196}Au and of ^{200m}Au, respectively. The 334-keV gamma line, however, exhibited a positive anisotropy, much larger than expected for the 333-keV gamma transition of ^{196}Pt. The positive anisotropy indicates a predominant dipole character with $I_i - I_f = +1$ for this transition in ^{198}Au. For the 180-keV gamma line a large negative anisotropy was found, showing that despite the underlying 181-keV gamma transition of ^{200}Hg (with negative anisotropy) the 180-keV gamma rays of ^{198}Au possess a negative anisotropy. This observation is in good agreement with the E2-multipolarity assigned to the 180-keV transition /10,11/.

The experimental anisotropy curves were lease-square fitted to the theoretical function /13/.

$$W(\Theta,T) = 1 + \sum_k B_k U_k F_k Q_k P_k(\cos\Theta)$$

where $P_K(\cos\Theta)$ are the Legendre polynominals, and Θ represents the angle between the direction of gamma ray emission and the quantization axis (in the present case identical to the direction of magnetization). The maximum value of k is determined by the spins of the nuclear states and by the gamma ray multipolarities. If parity-violating admixtures in the pertinent nuclear states and hence parity impurities in the gamma radiation field can be neglected, non-zero contributions to $W(\Theta,T)$ result only for even values of k. Therefore, only terms with $k = 2$ and $k = 4$ were taken into account in the present work. The F_K are the angular

distribution coefficients for the observed gamma transition, the U_k are parameters describing the reorientation due to unobserved preceding decays, and the Q_k correct for the finite solid angle of the detector. The orientation parameters B_k are statistical tensors which describe the population of the nuclear sublevels, depending on the ratio of the hyperfine interaction μH_{eff} to the thermal energy.

The anisotropy curve of the 204-keV gamma line (Fig. 3) was least-squares fitted with μH_{eff} and the E2/M1 mixing ratio δ (in the notation of Krane and Steffen[14]) as free adjustable parameters, assuming a spin of I = 12 for the isomeric state. The U_2 and U_4 coefficients were calculated on the basis of the decay scheme of Fig. 1. For the mixing ratio a value of $\delta_{204} = -0.10 \pm 0.05$ was obtained, confirming the almost pure dipole character of the 204-keV gamma transition.

In the least-squares fit of the 215-keV data for iron (Fig. 2) and nickel hosts the $\Theta = 0^\circ$ and $\Theta = 90^\circ$ spectra were fitted simultaneously, taking only μH_{eff} and an amplitude factor as free adjustable parameters and assuming again I = 12 for the isomeric state. The U_2 and U_4 coefficients were again calculated on the basis of the decay scheme of Fig. 1, taking our result for the mixing ratio δ_{204} into account. The fit result for the amplitude factor showed that the observed anisotropies are in quantitative agreement within 3% with the anisotropy values expected on the basis of the spin and multipolarity assignments of the proposed decay scheme (Fig. 1).

Although the interfering activities of ^{196}Au and ^{200m}Au did not allow a quantitative analysis of the anisotropies of the 180-keV and

334-keV gamma lines of ^{198m}Au, other gamma lines originating from these activities as well as the strong 412-keV gamma line following the decay of the ground state of ^{198}Au were used for testing the whole procedure of the present NO experiment. In particular the analysis of the temperature dependence of the reduced intensity of the 412-keV gamma line yielded perfect agreement with known values for the hyperfine interaction and the total anisotropy. This clearly indicates that the branching ratio of a possible β^- decay of ^{198m}Au into levels of ^{198}Hg, corresponding to the strong β^- branch in the decay of ^{200m}Au, must be rather small. A summary of the results for the magnetic hyperfine interaction μH_{eff} of ^{198m}Au in iron and nickel hosts resulting from the least-square fits of the various data is presented in Table 1, column 3. For a derivation of the magnetic moment we used the hyperfine fields determined for the β^- ground-state of ^{198}Au in iron /15/ and nickel /9/ by the NMR-ON technique; taking μH_{hf} = - 1158±1 kOe[16] for iron and H_{hf} = - 260.8±1.3 kOe for nickel as a host and accounting for the external polarizing field of 4 kOe, the values for the magnetic moment presented in column 4 are obtained. In Ref. 6 the hyperfine anomaly between the 2^- ground state and the 12^- isomeric state of ^{196}Au was estimated on the basis of the Bohr-Weisskopf theory /17/ as $^{196}\Delta^{196m}_{BW}$ = +2.3%. Applying this correction to the average of the two magnetic moment values obtained for iron and nickel hosts (listed in Table 1) we obtain as a final result

$$\mu = (+)\ 5.55\pm0.35 \text{ n.m.},$$

with the positive sign resulting from systematics.

IV. Discussion

The measured magnetic moment of 2.3-d ^{198m}Au is of quite similar magnitude as the moments of the 12^- states of ^{196}Au and ^{200}Au. A spin-parity assignment of 12^- seems therefore justified for ^{198m}Au, corresponding to a shell-model configuration of $[\pi h_{11/2};\ \nu i_{13/2}]\ 12^-$. The sign of the magnetic moment, which cannot be determined in nuclear orientation experiments of the present type, should then be assumed as positive. In Table 2 the values of the magnetic moments of the three 12^- gold isomers are summarized.

From the shell-model coupling rule, the magnetic moment of a $[\ h_{11/2};\ i_{13/2}\ ]12^-$ configuration is equal to the sum of the individual moments

$$\mu(12^-) = \mu(11/2^-) + \mu(13/2^+).$$

Experimental values are known for the magnetic moments of the $13/2^+$ states of the neighboring platinum, mercury, and lead isotopes /18/. The moments of the $13/2^+$ states in the mercury and lead isotopes are almost identical, differing by less than 0.05 n.m. from $\mu(13/2) \simeq -1.0$ n.m. Using this value for the neutron contribution to the magnetic moment of the 12^- states an $h_{11/2}$-proton moment is obtained, ranging from 6.4 n.m. (for ^{196m}Au) up to 7.1 n.m. (for ^{200m}Au).

With the core-polarization theory of Arima and Horie /19/ which represents a first-order correction to the single-particle moment, $\mu(11/2)_{s.p.} = 7.8$ n.m., one obtains a value of $\mu(11/2)_{corr.} = 6.7$ n.m. This value is almost independent of the assumed neutron number and is quite comparable to the above values derived from the experimental results.

On the other hand, the experimental values for the magnetic moments of the three 12^- states exhibit larger differences than one would expect for such high-spin states. Part of the differences might be due to the different neutron configurations of the three gold isotopes. This is supported by the fact that the $13/2^+$ state of ^{195}Pt has a magnetic moment smaller in magnitude by about 0.4 n.m. than those of the magnetic moments of the corresponding $13/2^+$ states of the neighboring mercury and lead isotopes.

For the $h_{11/2}$-proton component only one direct experimental magnetic moment result is known: the magnetic moment of the $11/2^-$ state of ^{191}Ir has been measured as $\mu(11/2) = 6.01 \pm 0.04$ n.m. /20/. If we subtract the neutron part (μ (13/2) $\simeq$ - 1.0 n.m.) from our results for the magnetic moments of ^{196m}Au, ^{198m}Au, and ^{200m}Au, proton contributions of 6.4 n.m., 6.5 n.m., and 7.1 n.m. are obtained. These are up to 1 n.m. larger than the magnetic moment of the $11/2^-$ state of ^{191}Ir. Only a fraction of these differences can be attributed to the additional proton pair in gold as compared to iridium, since the core-polarization theory predicts only a magnetic-moment difference of $\Delta\mu \simeq$ 0.3 n.m. due to the additional proton pair.

A possible cause for the decreasing $\pi h_{11/2}$ moments from ^{200m}Au to ^{191m}Ir could be given by second and higher-order effects of configuration mixing, including admixtures of collective states /21/. Since the magnitude of the moments would be reduced by such effects one would have to assume increasing higher-order effects from ^{200m}Au to ^{191m}Ir. This is not unreasonable in view of the fact that the electric quadrupole moment of the $3/2^-$ ground state of ^{197}Au is smaller by a factor of 2 than that

of the corresponding states in the iridium isotopes. A meaningful correction for such higher-order effects, however, can only be applied when the type of admixtures and their moment contributions are known.

Footnotes and References

†Present address: Hahn-Meitner Institut für Kernforschung, D-1 Berlin, Germany.

‡Present address: Abteilung für Physik und Astronomie, Ruhr-Universität Bochum, D-463 Bochum, Germany.

§Present address: General Electric Research and Development Center, Schenectady, New York.

1. C. M. Lederer, J. M. Hollander, and I. Perlman, Table of Isotopes, Sixth Edition (Wiley and Sons, New York, 1967).
2. R. Van Lieshout, R. Cirgis, R. A. Ricci, and A. H. Wapstra, Nucl. Phys. 25, 703 (1962).
3. Y. W. Chan, W. B. Ewbank, W. A. Nierenberg, and H. A. Shugart, Phys. Rev. 127, 572 (1962).
4. A. H. Wapstra, P. F. A. Goudsmit, J. F. W. Jansen, J. Konijn, K. E. G. Löbner, G. J. Nijgh, and S. A. deWit, Nucl. Phys. A93, 527 (1967).
5. B. Rosner, J. Felsteiner, H. Lindemann, and D. Zellermayer, Nucl. Phys. A172, 643 (1971).
6. F. Bacon, G. Kaindl, H.-E. Mahnke, and D. A. Shirley, Phys. Letters 37B, 181 (1971).
7. K. Sakai and P. J. Daly, Nucl. Phys. A118, 361 (1968).
8. J. C. Cunnane, R. Hochel, S. W. Yates, and P. J. Daly, Nucl. Phys. A196, 593 (1972).
9. F. Bacon, G. Kaindl, H.-E. Mahnke, and D. A. Shirley, Phys. Rev. C7, 1654 (1973).

10. J. C. Cunnane and P. J. Daly, Phys. Rev. C6, 1407 (1972).

11. A. Pakkanen, P. Puumalainen, H. Helppi, and T. Komppa, Nucl. Phys. A206, 164 (1973).

12. F. Bacon, G. Kaindl, H.-E. Mahnke, and D. A. Shirley, J. Phys. Soc. (Japan) 34 Suppl., 243 (1973).

13. R. J. Blin-Stoyle and M. A. Grace, Handbuch der Physik 42, 555 (Springer-Verlag, Berlin, 1957).

14. K. S. Krane and R. M. Steffen, Phys. Rev. C2, 724 (1970).

15. R. A. Fox and N. J. Stone, Phys. Letters 29A, 341 (1969).

16. In the original work of Ref. 15 the magnetic hyperfine field was derived using the magnetic moment uncorrected for diamagnetic shielding, whereas we have used the corrected value.

17. A. Bohr and V. F. Weisskopf, Phys. Rev. 77, 94 (1949).

18. V. S. Shirley, Table of Nuclear Moments, in Hyperfine Interactions in Excited Nuclei, edited by G. Goldring and R. Kalish (Gordon & Breach, New York, 1971), p. 1255.

19. A. Arima and H. Horie, Progr. Theor. Phys. 12, 623 (1954).

20. G. Eska, E. Hagn, T. Butz, P. Kienle, and E. Umlauf, Phys. Letters 36B, 328 (1971).

21. S. Nagamiya and T. Yamazaki, Phys. Rev. C4, 1961 (1971).

Table 1. Summary of magnetic-hyperfine interaction results for ^{198m}Au in iron and nickel, obtained from an analysis of the anisotropies of the gamma lines specified in column 2. In the last column the derived values for the magnetic moment of the isomeric state are listed.

Host	gamma line (keV)	$\lvert\mu H_{eff}\rvert$ (10^{-18} erg)	$\lvert\mu\rvert$ (n.m)
Fe	215	29.4±1.6	5.03±0.28
Ni	215	7.9±0.6	5.78±0.40
Ni	204	6.5±1.0	
		mean value	5.41±0.34

Table 2. Magnetic moments of the 12^- states of $^{196, 198, 200}Au$, corrected for hyperfine anomaly.

A	$T_{1/2}$ (h)	$\lvert\mu\rvert$ (n.m.)
196	9.7	5.35±0.20
198	55	5.55±0.35
200	18.7	6.10±0.20

Figure Captions

Fig. 1. Decay scheme of 2.3-d ^{198m}Au according to Ref. 10 and 11. The gamma ray energies and level energies are given in keV.

Fig. 2. Temperature dependences of the reduced intensities of the 215-keV gamma rays emitted parallel ($\theta = 0^{o}$) and perpendicular ($\theta = 90^{o}$) to the external polarizing field from a source of ^{198m}Au(Fe). The solid lines are the results of a simultaneous least-squares fit of both data sets.

Fig. 3. Reduced intensity of the 204-keV gamma rays at $\theta = 0^{o}$ from a ^{198m}Au(Ni) source versus inverse temperature.

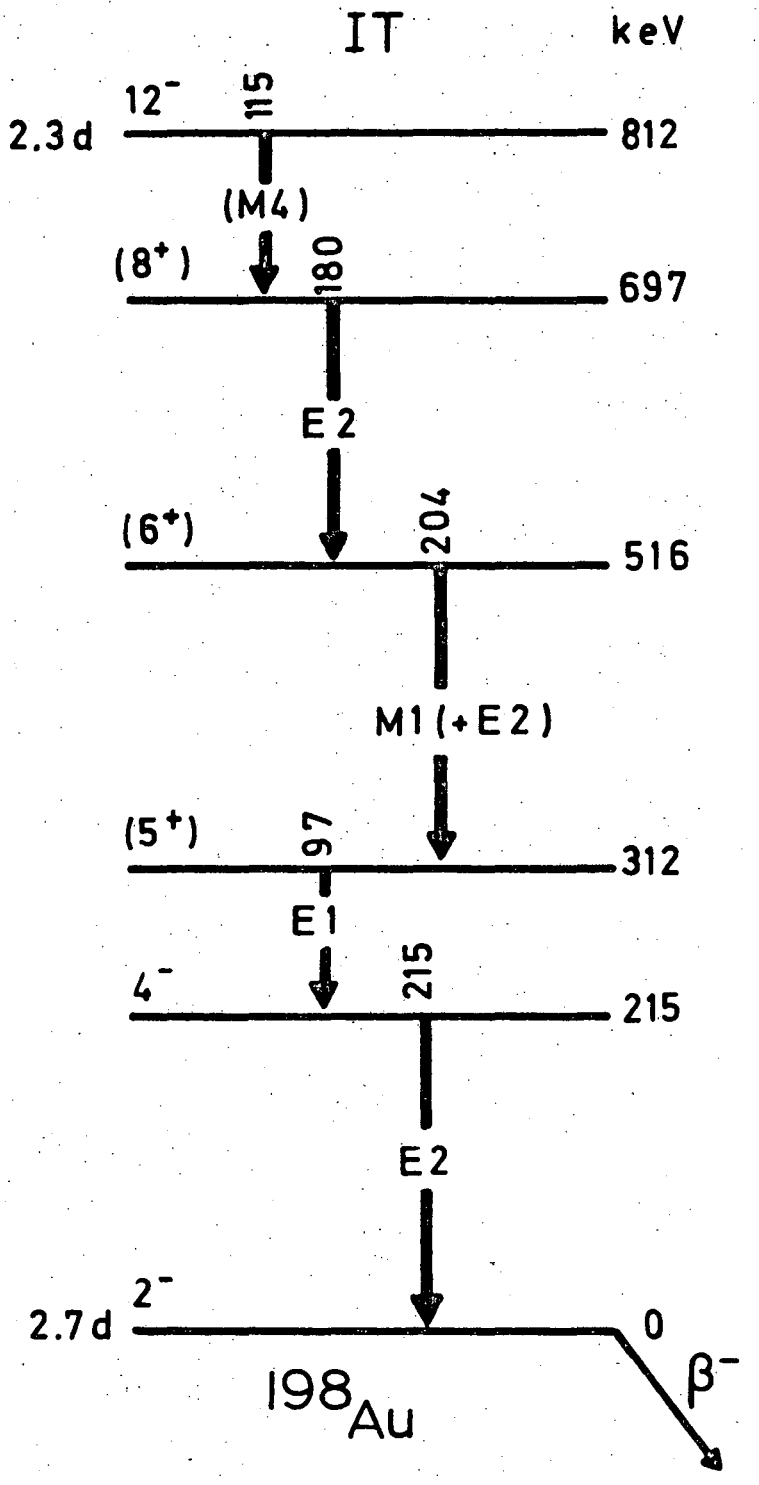
IT
keV
12⁻
115
2.3 d
812
(M4)
(8⁺)
180
697
E2
(6⁺)
204
516
M1 (+E2)
(5⁺)
97
312
E1
4⁻
215
215
E2
2⁻
2.7 d
0
β⁻
198Au
XBL 753-668

Fig. 1

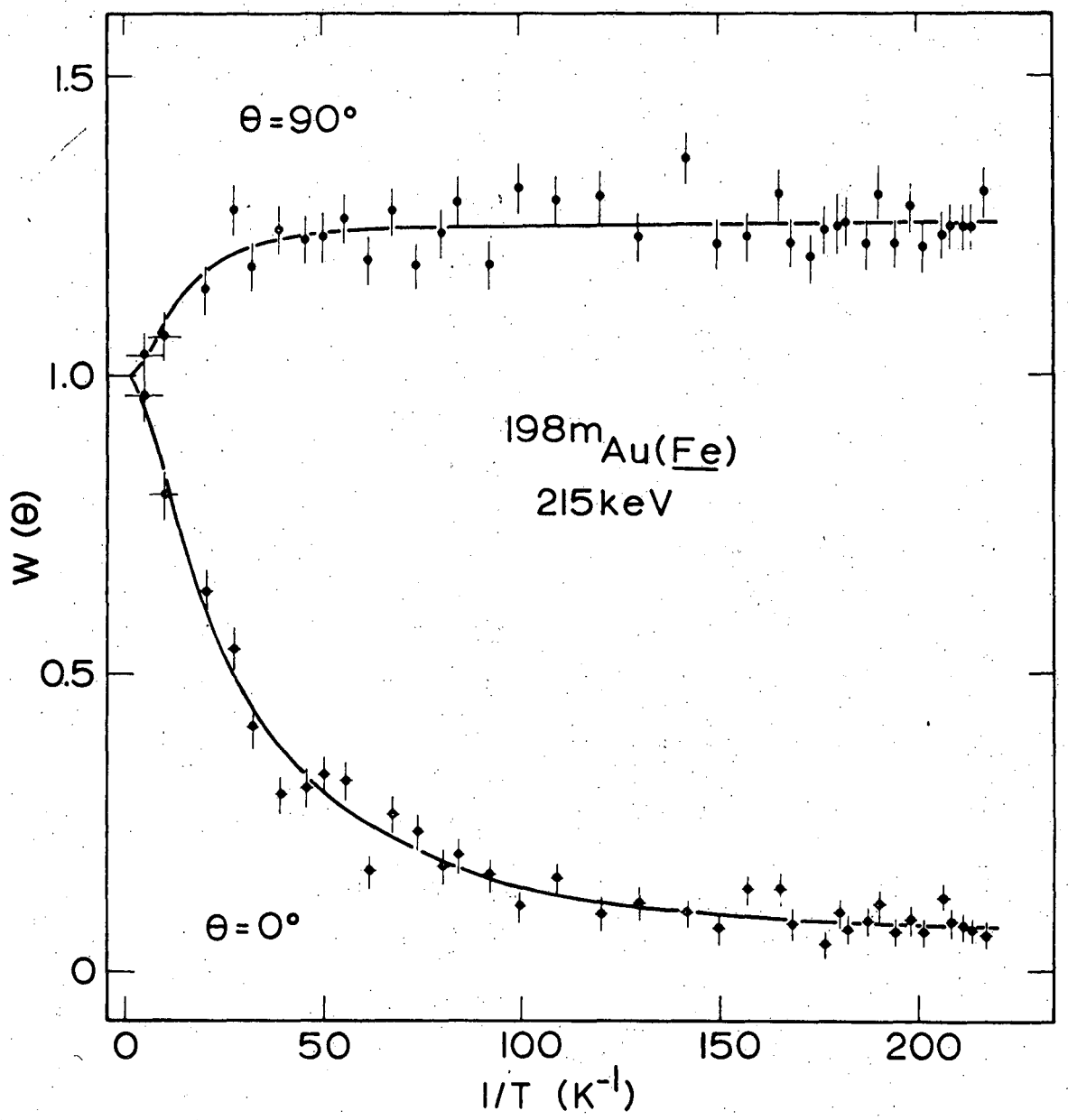

XBL 753-666

Fig. 2

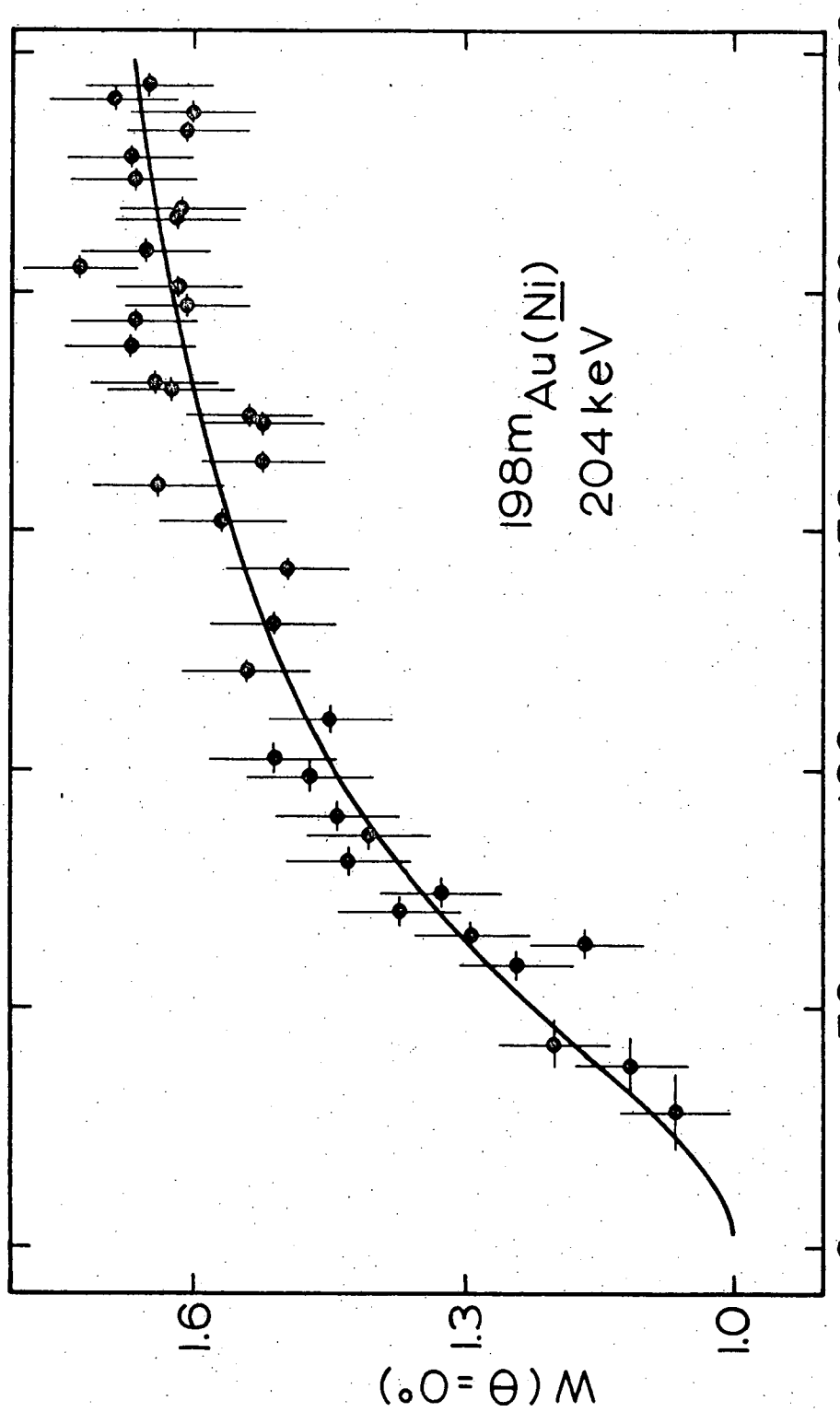

XBL 753-667

Fig. 3

TECHNICAL INFORMATION DIVISION
LAWRENCE BERKELEY LABORATORY
UNIVERSITY OF CALIFORNIA
BERKELEY, CALIFORNIA 94720